CrystEngComm

Accepted Manuscript

ROYAL SOCIETY OF CHEMISTRY

www.rsc.org/crystengcomm

Controllable synthesis and morphology evolution from two-dimension to one-dimension of layered $K_2V_6O_{16}\cdot nH_2O$

Xingang Kong[a*] Zhanglin Guo[a], Puhong Wen[b], Jianfeng Huang[a], Liyun Cao[a], Lixiong Yin[a], Jiayin Li[a], Qi Feng[c]

[a] School of Materials Science and Engineering, Shaanxi University of Science and Technology, Weiyang, Xi'an, Shaanxi 710021, PR China

[b] Department of Chemistry and Chemical Engineering, Baoji University of Arts and Science, 1 Gaoxin Road, Baoji, Shaanxi 721013, PR China

[c] Department of Advanced Materials Science, Faculty of Engineering, Kagawa University, 2217-20 Hayashi-cho, Takamatsu-shi, 761-0396 Japan

Abstract

The two-dimensional (2D) layered $K_2V_6O_{16}\cdot 2.7H_2O$ platelike single crystal was successfully synthesized in a short time of 3 h via a simple hydrothermal method. The crystal H_2O molecule number and morphology of layered $K_2V_6O_{16}\cdot nH_2O$ hexavanadate can be easily controlled by adjusting the system pH value and reaction time in the hydrothermal process. Through studying the structures and morphologies of the hexavanadate samples obtained at different reaction time under acid condition using X-ray diffractometer (XRD) and field emission scanning electron microscopy (FE-SEM), transmission electron microscope (TEM), it is concluded that the 2D layered $K_2V_6O_{16}\cdot 2.7H_2O$ platelike single crystal hexavanadate gradually evolves to the one-dimensional (1D) layered $K_2V_6O_{16}\cdot 1.5H_2O$ fiberlike single crystal hexavanadate in the hydrothermal process with prolonging the reaction time. In

* Corresponding author: Tel./fax: +86 029 86168802.

E-mail addresses: yezhu_1983@163.com (Xingang Kong).

addition, the photocatalytic performances of the as-prepared products were explored.

Key words: Hydrothermal synthesis, $K_2V_6O_{16}\cdot nH_2O$, Morphology evolution, Crystal growth, photocatalysis

1. Introduction

Layered structure compounds usually possess two-dimensional (2D) or one-dimensional (1D) structure morphology, such as the platelike $K_{0.8}Ti_{1.73}Li_{0.27}O_4$,[1] the platelike $K_4Nb_6O_{17}$,[2] the needle-like $K_2Ti_4O_9$,[3] and so on. Layered structure compounds are useful precursors for designing and preparing 1D or 2D hetero-/nanostructural materials in the soft chemical synthesis because of their ion-exchange properties, open structures and special morphologies.[4-8] At the same time they are typical functional materials that have been widely applied in various areas.[9-14]

The Hewettite $M_2V_6O_{16}\cdot nH_2O$ (M=monovalent element) vanadates, consisting of V_3O_8 layers and interstitial hydrated M ions, are series of layered compounds.[15] Researchers find that $M_2V_6O_{16}\cdot nH_2O$ hexavanadate have potential applications in areas such as high-energy lithium batteries, electrochromism, and chemical sensors.[16-18] The hydrous $M_2V_6O_{16}\cdot nH_2O$ hexavanadate can only be obtained by the wet chemical method, such as hydrothermal method,[19] homogeneous precipitation method,[20] sol-gel method,[21] and so on. For the hydrothermal synthesis of $K_2V_6O_{16}\cdot nH_2O$ and $Na_2V_6O_{16}\cdot nH_2O$, the temperature of 180 ^oC and the reaction time of 24 h were usually employed and the products all have the 1D shapes of wire and belt.[19, 22-26] The 1D $(NH_4)_2V_6O_{16}\cdot nH_2O$ nanorod was prepared for 24 h by Park et al. using the homogeneous precipitation method.[20] Among the literatures of layered $M_2V_6O_{16}\cdot nH_2O$ hexavanadate, reports about 1D morphology are common, whereas the layered $M_2V_6O_{16}\cdot nH_2O$ hexavanadate with 2D morphology is reported rarely.[21]

In this communication, we describe in detail the hydrothermal synthesis of 2D platelike

$K_2V_6O_{16}\cdot 2.7H_2O$ single crystal and the morphology evolution mechanism of $K_2V_6O_{16}\cdot nH_2O$ hexavanadate from platelike $K_2V_6O_{16}\cdot 2.7H_2O$ to fiberlike $K_2V_6O_{16}\cdot 1.5H_2O$ in the hydrothermal process. And the photocatalytic performances of $K_2V_6O_{16}\cdot 2.7H_2O$ and $K_2V_6O_{16}\cdot 1.5H_2O$ products were explored.

2. Experimental Section

0.05 g of V_2O_5 and 40 mL of 3 $mol\cdot L^{-1}$ KOH water solution were placed in a Teflon-lined autoclave with an inner volume of 100 mL, and stirred to form clear solution. Then the pH was adjusted to a desired value with 2 $mol\cdot L^{-1}$ HCl solution. After that, the mixture was solvothermally treated at 180 ^oC for a certain time under stirring conditions. After the hydrothermal treatment, the products were filtered and washed with distilled water, then dried at room temperature.

The crystal structure of the samples were characterized using a powder X-ray diffractometer (XRD, Rigaku D/max-2200PC) with Cu Kα (λ=0.15418 nm) radiation, field emission scanning electron microscopy (FE-SEM, Hitachi S-4800), transmission electron microscope (TEM, TecnaiG2F20S-TWIN), UV–vis absorption spectra were recorded on a UV/vis/NIR Spectrophotometer (LAMBDA950, PerkinElmer). The photocatalytic performances of samples were evaluated by degradation of methyl orange (MO), using PLS-SXE 300UV Xe lamp with a UV-cutoff (≥400nm) filter as the light source. In each experiment, 50 mg of samples were added into the solution (50 mL, 10 $mg\cdot L^{-1}$). The suspensions were magnetically stirred in dark for 40 min to ensure the establishment of an adsorption–desorption equilibrium. Then, the solution was exposed to the lamp irradiation under magnetic stirring. At different irradiation time intervals, 6 mL of the solution was collected with centrifugation. The concentration of the remnant dye in the collected solution was monitored by UV–vis spectroscopy (Unico UV-2600) each 30 min.

3. Result and discussion

In room temperature, V_2O_5 easily reacts with KOH, forming soluble K_3VO_4 potassium vanadate, then K_3VO_4 transforms to various potassium hexavanadate after hydrothermal teeatment at the conditions of different pH values. Fig. 1 shows the XRD patterns of the potassium hexavanadates obtained under hydrothermal condition of 180 ^oC for 6 h. At pH=1, no precipitate generates, and only yellow solution is obtained. The sample prepared at the condition of pH=2 presents the same diffraction peaks as that of $HNaV_6O_{16}\cdot 4H_2O$ (JCPDS No. 49-0996)(Fig. 1a), although there is not Na element in this reaction system. In consideration of the similar formation condition (At pH=2.75, the reported $HNaV_6O_{16}\cdot 4H_2O$ was obtained by hydrothermal reaction[27]) and the similar properties between Na and K element, therefore, we consider that the sample prepared at condition of pH=2 has a chemical formula of $HKV_6O_{16}\cdot 4H_2O$, which is a member of Hewettite $M_2V_6O_{16}\cdot nH_2O$ family. When the pH value is 3, a pure $K_2V_6O_{16}\cdot 1.5H_2O$ phase (JCPDS No. 51-0379) is formed (Fig. 1b), which is consistent with the literature.[19] The sample obtained at pH=4 displays the mixed phase of $K_2V_6O_{16}\cdot 1.5H_2O$ and $K_2V_6O_{16}\cdot 2.7H_2O$ (JCPDS No. 54-0602) (Fig. 1c). When the pH value increases to 6, a pure $K_2V_6O_{16}\cdot 2.7H_2O$ phase sample with fine crystallinity generates (Fig. 1d). When the pH value is 8, no precipitate is formed, and Vanadium still exists in the solution. These results indicate that these layered potassium hexavanadate products can be synthesized at hydrothermal conditions of pH=2~6. The number of crystal H_2O molecules and the species of cations between interlayers change with the pH value varies from 2 to 6, but the layered $V_3O_8^-$ framework structure is not influenced by the change of pH values.

The morphologies of the hexavanadate samples remarkably evolve with the change of pH value in the hydrothermal treatment. The $HKV_6O_{16}\cdot 4H_2O$ sample has a 1D wire shape with the size of about

200 nm in width and 3 μm in length (Fig. 2a), which is the same as that of the reported $HNaV_6O_{16}\cdot 4H_2O$.[19] The pure $K_2V_6O_{16}\cdot 1.5H_2O$ phase sample displays the fiberlike morphology with about 350 nm in width and 3-10 μm in length (Fig. 2b), which is consistent with the literature.[19] The pure $K_2V_6O_{16}\cdot 2.7H_2O$ phase sample shows 2D platelike morphology with about 50 μm in width and 100 μm in length (Fig. 2d). Two kinds of particles with fiberlike and platelike shapes are observed in the mixed phase sample (Fig. 2c), and corresponded to $K_2V_6O_{16}\cdot 1.5H_2O$ phase and $K_2V_6O_{16}\cdot 2.7H_2O$ phase, respectively. This is accordant with XRD pattern.

The TEM images also indicate that the pure $K_2V_6O_{16}\cdot 2.7H_2O$ and pure $K_2V_6O_{16}\cdot 1.5H_2O$ phase show uniform 2D plate-like and 1D fiber morphology (Fig. 3a and c), respectively. In SAED pattern of $K_2V_6O_{16}\cdot 2.7H_2O$ sample (Fig. 3b), the d-values of diffraction spots are 0.82nm and 0.49 nm, which corresponded to the (010) and (001) planes of the $K_2V_6O_{16}\cdot 2.7H_2O$ phase, respectively, implying the exposed facet the $K_2V_6O_{16}\cdot 2.7H_2O$ plate is (100)-plane. In SAED pattern of $K_2V_6O_{16}\cdot 1.5H_2O$ sample (Fig. 3d), the d-value of diffraction spots are 0.34nm and 0.59 nm, which correspond to the (010) and (200) planes of the $K_2V_6O_{16}\cdot 1.5H_2O$, respectively, indicating the axis direction of single fiber is b-axis direction and the dominant exposing fates is (001) and (100) facets. In fact, when we observe the HRTEM images and SAED patterns of the samples, we find that the $K_2V_6O_{16}\cdot 2.7H_2O$ and $K_2V_6O_{16}\cdot 1.5H_2O$ samples easily transform into amorphous phase from crystalline phase during irradiating with the strong electron beam and, as shown in Fig. 4. HRTEM images of $K_2V_6O_{16}\cdot 2.7H_2O$ plate (Fig. 4a and b) were taken from the same position in the interval of about 5 seconds, and have the remarkably difference. The interplanar distances observed in Fig. 4a and b are the same and are respectively corresponding to (100) and (110) facets, but crystalline phase changes into amorphous phase during electron beam irradiation, and the amorphous area clearly enlarged in the same position of

$K_2V_6O_{16}·2.7H_2O$ plate. The same phenomenon is also detected in the HRTEM images and SAED patterns of $K_2V_6O_{16}·1.5H_2O$ samples. The crystal lattice fringes of (10-1) facet and the distinct diffraction spots can all be observed in Fig. 4c, however, after the strong electron beam irradiates the same position of $K_2V_6O_{16}·1.5H_2O$ samples for several seconds, the crystal lattice fringes can't be observed in its HRTEM image, and its SAED pattern displays the diffraction rings, but not the diffraction points (Fig. 4d). These indicate that similar to other compounds that had been reported,[28] these hydrous layered $K_2V_6O_{16}·nH_2O$ potassium hexavanadates are unstable under the strong electron beam irradiation condition, leading to the destruction of their crystalline.

Moreover, it is discovered that the surface of platelike particles among the mixture produced under hydrothermal condition of pH=4 at 180 °C for 6 h is very rough, and part of this platelike particle has broken up into fibers through the distinct observation of high magnification FE-SEM (Fig. 5b), and we regard these fibers as the $K_2V_6O_{16}·1.5H_2O$ phase, meanings the $K_2V_6O_{16}·1.5H_2O/K_2V_6O_{16}·2.7H_2O$ composite. Therefore, to research the morphology evolution mechanism of samples obtained in hydrothermal process, we respectively set the hydrothermal time for 1 h, 3 h and 12 h at condition of pH=4 and 180 °C. After the hydrothermal reaction for 1 h, almost no precipitate produced. After the hydrothermal reaction under the condition of pH=4 at 180 °C for 3 h and 12 h, respectively, XRD analysis (Fig. S1) indicate that the prepared products display the almost pure $K_2V_6O_{16}·2.7H_2O$ phase and the pure $K_2V_6O_{16}·1.5H_2O$ phase, respectively. FE-SEM images show that this $K_2V_6O_{16}·2.7H_2O$ particle presents a smooth platelike morphology (Fig. 5a) and the $K_2V_6O_{16}·1.5H_2O$ sample possesses the fiberlike shape Fig. 5c). These results suggest that the 1D $K_2V_6O_{16}·nH_2O$ particle with crystal H_2O n=1.5 is steadier than that with n=2.7 under the hydrothermal condition. It is indicated that the Hewettite $K_2V_6O_{16}·nH_2O$ can be produced in a short time under the acid hydrothermal system. The

shape of $K_2V_6O_{16}\cdot nH_2O$ hexavanadate evolves from 2D structure to 1D structure with prolonging the hydrothermal time, and its crystal H_2O number decreases from 2.7 to 1.5, whereas the layered Hewettite $K_2V_6O_{16}\cdot nH_2O$ structure is remained. In most literatures,[19, 22-26] the hydrothermal time is more than 24 h for the preparation of $M_2V_6O_{16}\cdot nH_2O$ hexavanadate, which leads to that the samples all present 1D structure shape, but not 2D morphology. In addition, in the hydrothermal system of pH=6 at 150 °C, we operated respectively the hydrothermal time for 3h, 6h, 12h and 24h, and also obtained the pure platelike $K_2V_6O_{16}\cdot 2.7H_2O$ particles, mixture of platelike $K_2V_6O_{16}\cdot 2.7H_2O$ and fiberlike $K_2V_6O_{16}\cdot 1.5H_2O$ particles and pure fiberlike $K_2V_6O_{16}\cdot 1.5H_2O$ particles, respectively (Fig. S2 and S3). In the hydrothermal system of pH=3 at 200 °C, after the hydrothermal reaction for 3~12h, the obtained $K_2V_6O_{16}\cdot 1.5H_2O$ samples all show the fiberlike morphology (Fig. S4 and S5). In summary, in the hydrothermal systems, the pH value, reaction time and temperature are significant factors that influence the particle morphology of final product.

On the basis of above results, we propose a probable morphology evolution mechanism to explain the shape evolution of layered potassium hexavanadates from 2D structure to 1D structure, as shown in Fig. 5d. The hydrothermal synthesis of layered $K_2V_6O_{16}\cdot nH_2O$ can be divided into two stages. The first stage is a dissolution-crystallization process, in which $[VO_4]^{3-}$ ions transform into $[V_3O_9]^{3-}$ ions under hydrothermal condition of pH=3~6,[20, 27] and then $[V_3O_9]^{3-}$ ions gather and mainly grow into the $V_3O_8^-$ layers along 2D direction according to their growth habits, forming 2D platelike $K_2V_6O_{16}\cdot 2.7H_2O$ particles. The second stage is a fragmentation process, but not a redissolution-precipitation process. With extending the hydrothermal time, part of platelike $K_2V_6O_{16}\cdot 2.7H_2O$ particles gradually split into $K_2V_6O_{16}\cdot 1.5H_2O$ fibers to form the $K_2V_6O_{16}\cdot 1.5H_2O/2.7H_2O$ composite (Fig. 5b). With continuously prolonging the hydrothermal time, this composite thoroughly splits and transforms into the

$K_2V_6O_{16}·1.5H_2O$ fibers (Fig. 5c). Because we did not capture the TEM image and SAED patterns of $K_2V_6O_{16}·1.5H_2O/2.7H_2O$ composite, we can't confirm that the $K_2V_6O_{16}·2.7H_2O$ plate splits into the $K_2V_6O_{16}·1.5H_2O$ fiber along which direction ([010] or [001]) of $K_2V_6O_{16}·2.7H_2O$ phase. But we can affirm that there is a homologous relation between the (001) facet of $K_2V_6O_{16}·1.5H_2O$ and the (100) facet of $K_2V_6O_{16}·2.7H_2O$ through the XRD, TEM and SAED results discussed above.

Fig. 6a shows the UV-vis diffuse reflectance spectra of the pure $K_2V_6O_{16}·2.7H_2O$ plate and pure $K_2V_6O_{16}·1.5H_2O$ fiber samples obtained respectively under the conditions of pH=6 and 3 at 180 ^oC for 6 h. It can be seen that both $K_2V_6O_{16}·2.7H_2O$ and $K_2V_6O_{16}·1.5H_2O$ display the absorption edges in the ultraviolet light region of 350~420 nm and the visible light region of 450~510 nm. But they are different in the absorbance intensity, and respectively show the shiny yellow and brown color (Fig. 6). The band-gap of $K_2V_6O_{16}·2.7H_2O$ and $K_2V_6O_{16}·1.5H_2O$ are calculated to be 2.15 eV and 2.20 eV, respectively, that is to say that both of them using as photocatalysts can response to visible light. The photocatalytic performances of $K_2V_6O_{16}·2.7H_2O$ and $K_2V_6O_{16}·1.5H_2O$ samples were evaluated by degradation of MO solution under xenon lamp irradiation, respectively. Fig. 6b displays the temporal evolution of the spectral changes during the photodegradation of MO over $K_2V_6O_{16}·2.7H_2O$ sample under visible light irradiation. It can be seen that the absorbance of MO at the maximum absorption wavelength (463 nm) was gradually decreased with the prolongation of the irradiation time, indicating the destruction of MO chromophoric structure.[29] As shown in the Fig. 6c, the $K_2V_6O_{16}·1.5H_2O$ fiber sample shows stronger absorbance ability during dark reaction, because of its smaller particle size than that of $K_2V_6O_{16}·2.7H_2O$ plate. The $K_2V_6O_{16}·2.7H_2O$ and $K_2V_6O_{16}·1.5H_2O$ samples reach to the photocatalytic degradation efficiency of 35% and 40.1% for MO after visible irradiation for 90min. The photocatalytic performances of these two samples are not high and almost have no difference. This

indicates that comparing with the exposed (001) and (100) facets of $K_2V_6O_{16}\cdot 1.5H_2O$, the exposed (100) facet (basal plane) of $K_2V_6O_{16}\cdot 2.7H_2O$ platelike particle doesn't contribute to photocatalytic reaction.[30] Herein, the detailed photocatalytic mechanism of $K_2V_6O_{16}\cdot 2.7H_2O$ and $K_2V_6O_{16}\cdot 1.5H_2O$ is not discussed.

4. Conclusions

The layered Hewettite $K_2V_6O_{16}\cdot 2.7H_2O$ single crystal particle with 2D platelike morphology was successfully synthesized by controlling the pH value, reaction time and temperature in the hydrothermal process. Results show that the $K_2V_6O_{16}\cdot nH_2O$ platelike single crystal particles can be produced in a short time under the acid hydrothermal system, its 2D platelike shape evolves into 1D fiberlike shape with extending the hydrothermal time. Moreover, these two kinds of $K_2V_6O_{16}\cdot nH_2O$ samples display certain activities in photodegrading MO under visible light.

Acknowledgments

The authors acknowledgment the support of Project Supported by Natural Science Basic Research Plan in Shaanxi Province of China (Program No. 2013JQ6012), China Postdoctoral Science Foundation (Program No. 2013M542314), the research starting foundation from Shaanxi University of Science and Technology (BJ12-22), the Natural Science Foundation of China (No. 21173003& No. 51472153), and Innovation Team Assistance Foundation of Shaanxi Province (Grant No. 2013KCT-06).

References

[1] Q. Feng, M. Hirasawa and K. Yanagisawa, *Chem. Mater*., 2001, **13**, 290.

[2] X. Kong, D. Hu, P. Wen, T. Ishii, Y. Tanaka, Q. Feng, *Dalton Trans*., 2013, **42**, 7699.

[3] M. Allen, A. Thibert, E. Sabio, N. Browning, D. Larsen, F. Osterloh, *Chem. Mater*., 2009, **22**, 1220.

[4] X. Kong, D. Hu, Y. Ishikawa, Y. Tanaka, Q. Feng, *Chem. Mater*., 2011, **23**, 3978.

[5] X. Kong, Y. Ishikawa, K. Shinagawa, Q. Feng, *J. Am. Ceram. Soc*., 2011, **94**, 3716.

[6] W. Bi, Z. Hu, X. Li, C. Wu, J. Wu, Y. Wu, Y. Xie, *Nano Res*., 2014, 1-8.

[7] X. Kong, Z. Guo, P. Wen, L. Cao, J. Huang, C. Li, J. Fei, F. Wang, Q. Feng, *RSC Adv*., 2014, **4**, 56637.

[8] L. Cao, Z. Guo, J. Huang, C. Li, J. Fei, Q. Feng, P. Wen, Y. Sun, X. Kong, *Mater. Lett*., 2014, **137**, 110.

[9] S. Burkov, O. Zolotova, B. Sorokin, P. Turchin, *Ultrason*., 2015, **55**, 104.

[10] M. Cuddy, K. Arkill, Z. Wang, H. Komsa, A. Krasheninnikov, R. Palmer, *Nanoscale*, 2014, **6**, 12463.

[11] R. Layek, A. Das, M. Park, N. Kim, J. Lee, *J. Mater. Chem. A*, 2014, **2**, 12158.

[12] B. Lu, Y. Zhu, *Phys. Chem. Chem. Phys*., 2014, **16**, 16509.

[13] L. Dai, Y. Zhu, C. Jiao, Z. Sun, S. Shi, W. Zhou, M. Ma, *CrystEngComm*, 2014, **16**, 5050.

[14] S. Zhang, Z. Yan, Y. Li, Z. Chen, H. Zeng, *Angew. Chem. Int. Ed.*, 2015, **54**, 3112.

[15] Y. Oka, T. Yao, N. Yamamoto, O. Tamada, *Mater. Res. Bull.*, 1997, **32**, 59.

[16] P. Poizot, S. Laruelle, S. Grugeon, L. Dupont, J. Tarascon, *Nature*, 2000, **407**, 496.

[17] J. Livage, D. Ganguli, *Sol. Energy Mater. and Sol. Cells*, 2001, **68**, 365.

[18] J. Liu, X. Wang, Q. Peng, Y. Li, *Adv. Mater.*, 2005, **17**, 764.

[19] L. Bai, Y. Xue, J. Zhang, B. Pan, C. Wu, *Eur. J. Inorg. Chem.*, 2013, **2013**, 3497.

[20] H. Park, K. Kim. *Solid State Ionics*, 2010, **181**, 311.

[21] N. Steunou, C. Mousty, O. Durupthy, C. Roux, G. Laurent, C. Simonnet-Jégat, T. Coradin, *J. Mater. Chem.*, 2012, **22**, 15291.

[22] J. Yu, J. Yu, W. Ho, L. Wu, X. Wang, *J. Am. Chem. Soc.*, 2004, **126**, 3422.

[23] D. Zhou, S. Liu, H. Wang, G. Yan, *J. power. sources*, 2013, **227**, 111.

[24] G. Zhou, X. Wang, J. Yu, *Cryst. Growth Des.*, 2005, **5**, 969.

[25] P. Chithaiah, G. Chandrappa, J. Livage. *Inorg. Chem.*, 2012, **51**, 2241.

[26] Y. Xue, X. Zhang, J. Zhang, J. Wu, Y. Sun, Y. Tian, Y. Xie, *J. Mater. Chem.*, 2012, **22**, 2560.

[27] V. Channu, R. Holze, I. Yeo, S. Mho, R. Kalluru, *Appl. Phys. A*, 2011, **104**, 707.

[28] Q. Gu, K. Zhu, J. Liu, P. Liu, Y. Cao, J. Qiu, *RSC Adv.*, 2014, **4**, 15104.

[29] L. Yu, J. Xi, H. Chan, T. Su, D. Phillips, W. Chan, *Phys. Chem. Chem. Phys.*, 2012, **14**, 3589.

[30] K. Zhou, Y. Li, *Angew. Chem. Int. Ed.*, 2011, **50**, 2.

Figure Captions:

Fig. 1 XRD patterns of samples obtained at the hydrothermal condition of 180 ^{o}C for 6 h at different pH value. (a) pH=2, (b) pH=3, (c) pH=4, (d) pH=6.

Fig. 2 FE-SEM images of samples obtained at the hydrothermal condition of 180 ^{o}C for 6 h at different pH value. (a) pH=2, (b) pH=3, (c) pH=4, (d) pH=6.

Fig. 3 TEM images and SAED patterns of $K_2V_6O_{16}\cdot 2.7H_2O$ plate (a, b) and $K_2V_6O_{16}\cdot 1.5H_2O$ fiber (c, d).

Fig. 4 HRTEM images of the same position in the $K_2V_6O_{16}\cdot 2.7H_2O$ plate before(a) and after(b) irradiating with electron beam for 5 seconds. HRTEM image and SAED pattern (c) of the same position in the $K_2V_6O_{16}\cdot 1.5H_2O$ fiber before(a) and after(b) irradiating with electron beam for 5 seconds.

Fig. 5 FE-SEM images of samples obtained at the hydrothermal condition of pH=4 at 180 ^{o}C for 3h(a), 6h(b), 12h(c). Schematic diagram of morphology evolution(d).

Fig. 6 UV–visible diffuse reflectance spectra(a), time-dependent UV-vis absorption spectra of the MO solution in the presence of the $K_2V_6O_{16}\cdot 2.7H_2O$ sample(b), and photocatalytic degradation for MO results(c).

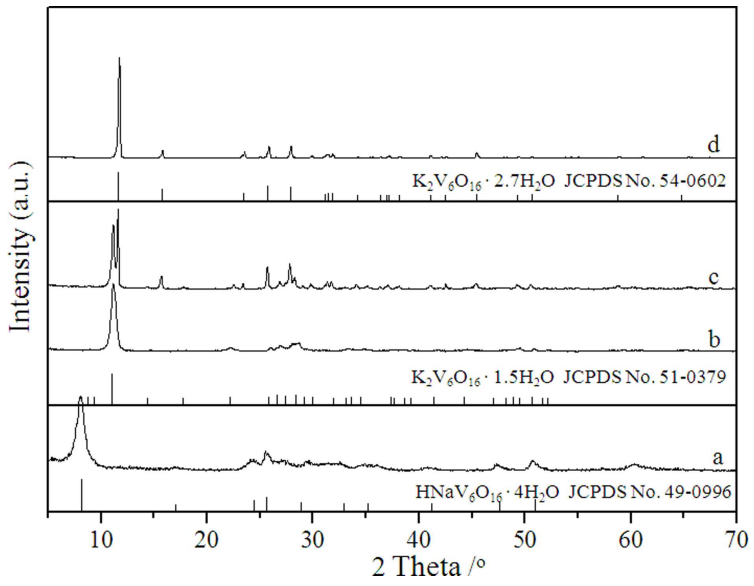

Fig. 1 XRD patterns of samples obtained at the hydrothermal condition of 180 °C for 6 h.(a) pH=2, (b) pH=3, (c) pH=4, (d) pH=6.

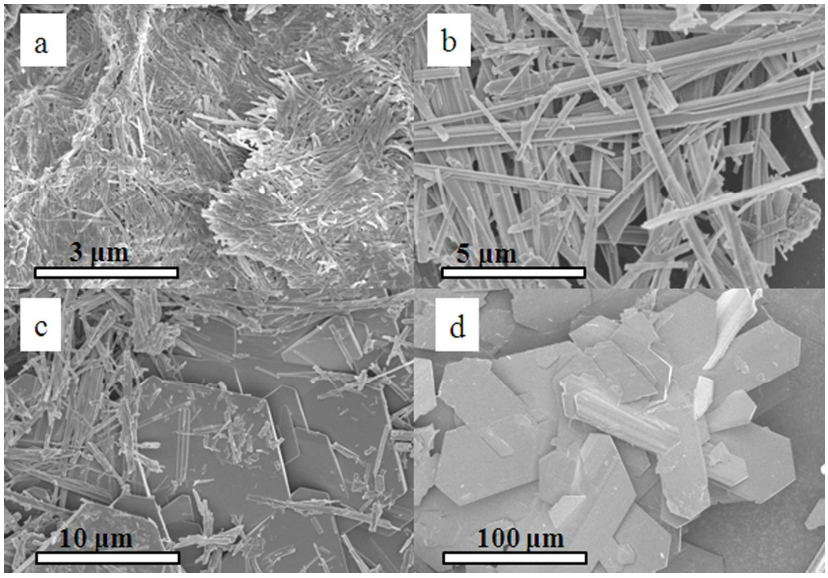

Fig. 2 FE-SEM images of samples obtained at the hydrothermal condition of 180 °C for 6 h. (a) pH=2, (b) pH=3, (c) pH=4, (d) pH=6.

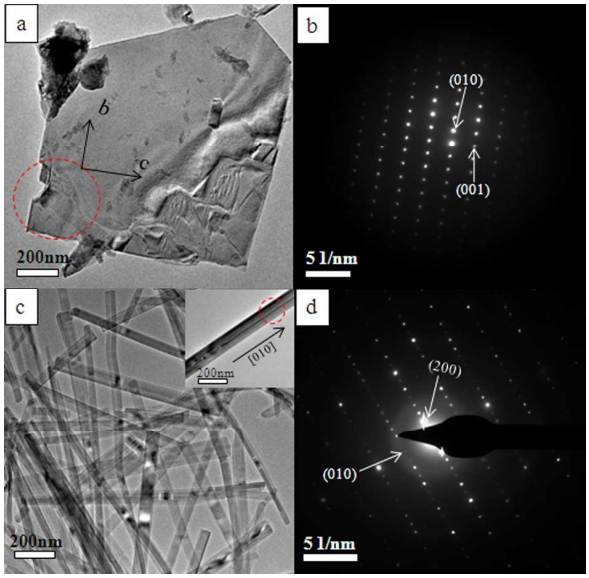

Fig. 3 TEM images and SAED patterns of $K_2V_6O_{16}\cdot 2.7H_2O$ plate (a, b) and $K_2V_6O_{16}\cdot 1.5H_2O$ fiber (c, d).

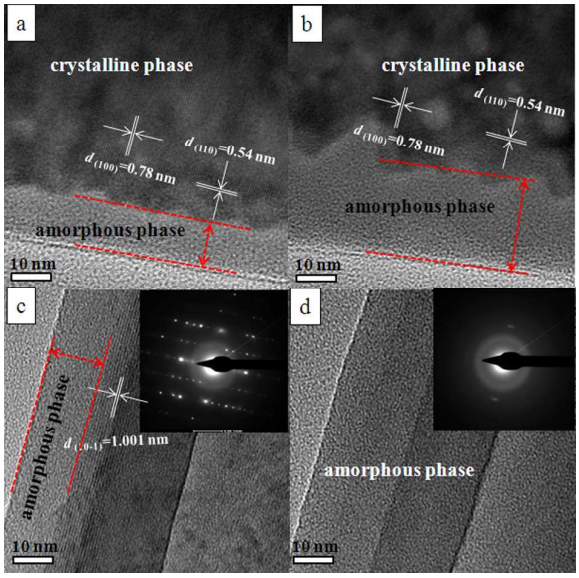

Fig. 4 HRTEM image(a) of $K_2V_6O_{16}\cdot 2.7H_2O$ plate, HRTEM image(b) of the same position as (a) after irradiating with electron beam for 5 seconds. HRTEM image and SAED pattern (c) of $K_2V_6O_{16}\cdot 1.5H_2O$ fiber, HRTEM image and SAED pattern (d) of the same position as (c) after irradiating with electron beam for 5 seconds.

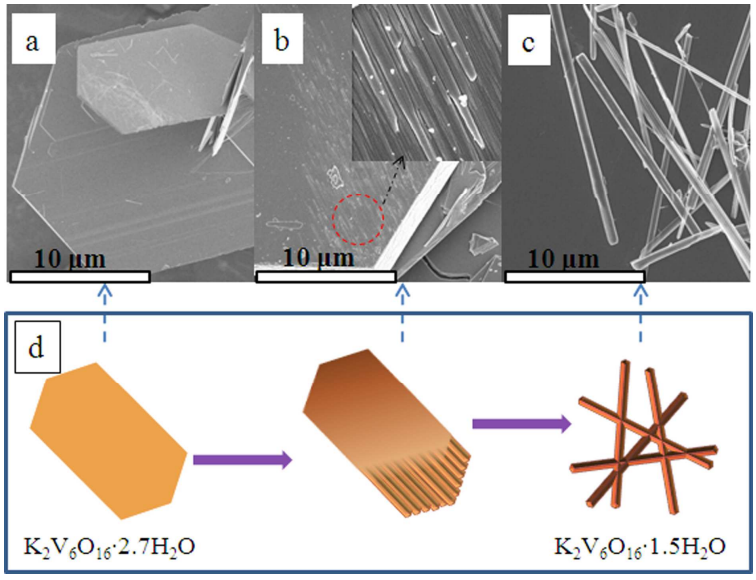

Fig. 5 FE-SEM images of samples obtained at the hydrothermal condition of pH=4 at 180 ^{o}C for 3 h(a), 6 h(b), 12 h(c). Schematic diagram of morphology evolution(d).

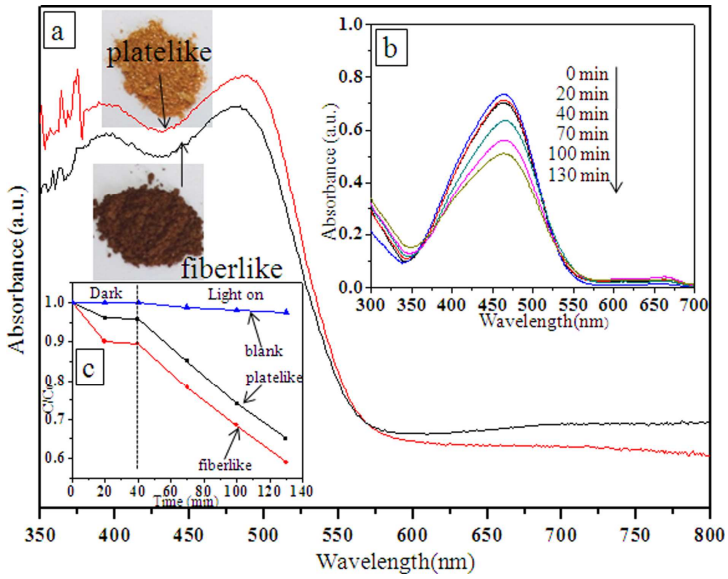

Fig. 6 UV–visible diffuse reflectance spectra(a), time-dependent UV-vis absorption spectra of the MO solution in the presence of the $K_2V_6O_{16}\cdot 2.7H_2O$ sample(b), and photocatalytic degradation for MO results(c).

Title: Controllable synthesis and morphology evolution from two-dimension to one-dimension of layered $K_2V_6O_{16}\cdot nH_2O$ and their photocatalytic properties

Author: Xingang Kong*, Zhanglin Guo, Puhong Wen, Jianfeng Huang, Liyun Cao, Lixiong Yin, Jiayin Li, Qi Feng

The table of contents entry: In the hydrothermal process, the layered $K_2V_6O_{16}\cdot 2.7H_2O$ platelike crystals split into layered $K_2V_6O_{16}\cdot 1.5H_2O$ fiberlike crystals.

ToC figure :